UICC
global cancer control

IJC
International Journal of Cancer

Imatinib response in two GIST patients carrying two hitherto functionally uncharacterized PDGFRA mutations: an imaging, biochemical and molecular modeling study

Palma Dileo[1], Sabrina Pricl[2], Elena Tamborini[3], Tiziana Negri[3], Silvia Stacchiotti[1], Alessandro Gronchi[4], Paola Posocco[2], Erik Laurini[2], Paola Coco[1], Elena Fumagalli[1], Paolo G. Casali[1] and Silvana Pilotti[3]

[1] Department of Medical Oncology, S.S. Trattamento Medico dei Sarcomi dell'Adulto, Fondazione IRCCS — Istituto Nazionale Tumori, Milano; Italy
[2] Department of Chemical, Environmental, and Raw Materials Engineering (DICAMP), Molecular Simulation Engineering (MOSE) Laboratory, University of Trieste, Italy
[3] Department of Pathology, Experimental Molecular Pathology, Fondazione IRCCS Istituto Nazionale dei Tumori di Milano; Italy
[4] Department of Surgery, Unità-Melanomi Sarcomi, Fondazione IRCCS Istituto Nazionale dei Tumori di Milano; Italy

Beside the well known "*in vivo*" and "*in vitro*" Imatinib resistant D842V mutation in PDGFRA receptor, very few are the information concerning the "*in vivo*" Imatinib activity with respect to the other PDGFRA mutations for which only "*in vitro*" data are available. Two patients carrying *PDGFRA* mutations in exons 18 (involving residues DIMH842-845) and 12 (V561D), respectively, were treated with Imatinib at a dose of 400 mg/day. According to Response Evaluation Criteria in Solid Tumors criteria, after a median treatment of 7 months both patients showed clinical partial response, and underwent surgery of the minimal residual disease. Tumor response was confirmed pathologically. In both patients, analyses of PDGFRA performed on pre- and/or post-treatment material were compared to affinity data of the mutated receptor towards the inhibitor. Molecular modeling evidence was found to be consistent with sensitivity of mutated PDGFRA receptors to Imatinib. Thus, the "*in vivo*" evidence that these two mutations of PDGFRA are sensitive to Imatinib was confirmed by a multidimensional approach comprising "*in silico*" experiments that, in association to molecular and biochemical analyses, constitutes a powerful tool to predict Imatinib sensitivity, clinically beneficial in the treatment of these tumors with molecularly targeted therapies.

Gastrointestinal stromal tumors (GISTs) are the most common mesenchymal tumors of the gastrointestinal tract. Nearly 90% of GISTs are marked by gain-of-function mutations in *KIT* tyrosine kinase, most frequently located at Exons 11 and 9 and, to a minor extent, at Exons 13 or 17. In the absence of *KIT* mutations, GISTs can harbor mutations of the *PDGFRA* gene,[1–4] mainly located at Exons 12, 18 and 14.

Recent studies have shown that the type and nature of *KIT* or *PDGFRA* mutations correlate with the clinical response to imatinib-mesylate (already known as Gleevec-Glevec; Novartis, Basel, Switzerland). GISTs with the most common *KIT* Exon 11 mutations show the highest response rates, whereas the responsiveness of those with *KIT* mutated in Exon 9 appears to be sensitive to the drug dose. Anyhow, response to imatinib closely correlates with the presence and type of *KIT* mutations. GISTs lacking mutations in *KIT*/*PDGFRA* show much lower response rates to imatinib, if no response at all. Finally, for the most common *PDGFRA* mutation in GISTs, the missense D842V substitution in Exon 18, there is evidence of insensitivity to imatinib.[4]

Herein, we report the efficacy of imatinib in two patients with mutations in the *PDGFRA* gene involving Exons 18 and 12, respectively. Molecular modeling results are also provided as a supporting rationale.

Key words: GIST, PDGFRA, Imatinib-mesylate, targeted therapy
Dr. Casali, Dileo, Stacchiotti, Fumagalli and Coco have been involved, as principal investigator and subinvestigators, in clinical trials sponsored by Novartis and Pfizer. Dr. Casali has received honoraria and travel coverage for medical meetings from Novartis and honoraria from Pfizer. Dr. Gronchi has received honoraria and travel coverage for medical meetings from Novartis.
The first two authors equally contributed to the work.
Grant sponsor: Associazione Italiana Ricerca sul Cancro (AIRC) grants (to S.P. and E.T.)
DOI: 10.1002/ijc.25418
History: Received 23 Dec 2009; Accepted 17 Mar 2010; Online 27 Apr 2010
Correspondence to: Palma Dileo, MD, S.S. Trattamento Medico dei Sarcomi dell'Adulto, Medical Oncology; Fondazione IRCCS—Istituto Nazionale Tumori, Via Venezian 1—20133 Milano; Italy, Tel.: +[39 0223902803], Fax: +[39 0223902804], E-mail: palma.dileo@istitutotumori.mi.it

Material and Methods

Clinical history

Patient A. On December 2000, a 61-year-old woman presented with mild abdominal discomfort and a 3-cm nodule (> 5/HPF) in the context of the gastric wall plus a 2.4-cm nodule in the right kidney, which were removed elsewhere.

Short Report

Pathologic report revealed a sporadic angiomyolipoma of the kidney, as long as an intermediate-risk gastric GIST.

A massive recurrent tumor in the stomach (24 cm) was excised in February 2006. At that time, the patient underwent gastrectomy and partial omentectomy. Postoperative staging, including whole-body computed tomography (CT) scan and fluorodeoxyglucose positron emission tomography (FDG-PET), was negative. Shortly after (August 31, 2006), the patient presented with tumor relapse, CT and PET scans revealing a peritoneal mass of 55 mm. At that time, the patient was started on imatinib (400 mg once daily). Toxicity was assessed at follow-up visits every 2 to 4 weeks, and blood-cell counts and blood chemical values were analyzed every 1 to 2 weeks. The response to treatment was assessed by whole-body CT scan and FDG-PET after the first and third month of treatment, then with whole-body CT scan every other month.

The patient was scheduled to surgery of the residual disease after 8 months of treatment. Before surgery, she underwent disease assessment by whole-body CT and PET scans.

Patient B. On June 2006, an asymptomatic 56-year-old man without any relevant medical history was admitted with a painless enlargement in his abdomen. Ultrasound and CT scans showed a 23-cm central abdominal mass. An ultrasound-guided biopsy was taken, providing a diagnosis of GIST. The lesion was deemed resectable only by an extensive abdominal procedure, requiring the excision of all adjacent organs (stomach, spleen, pancreas and possibly bowels). Given this, and the high risk of relapse even after complete surgery, the patient was offered a preoperative treatment with imatinib to improve the resectability of the lesion and possibly reduce the extension of the procedure. Disease assessment, including CT and PET scans, was done before starting imatinib. Then, he was started on imatinib (400 mg once daily). Response to treatment was assessed by whole-body CT scan and FDG-PET after the first month; whole-body CT scans were then performed every other month. The patient was scheduled to surgery of the residual disease after 6 months of treatment. Before surgery, he underwent disease assessment by whole-body CT and PET scans.

Tumor characterization

Radiologic evaluations. Radiologic evaluation was done according to Response Evaluation Criteria in Solid Tumors criteria, which have been introduced to unify response assessment criteria, to define how to choose evaluable lesions and to enable the use of new imaging technologies (spiral CT and magnetic resonance imaging).

Immunohistochemistry. The immunohistochemical analyses were made using 2-μm, formalin-fixed and paraffin-embedded tumoral sections of the surgical specimens and biopsy, using antibodies against CD117, PDGFRA, Ki-67 and desmin, as described previously,[5,6] and DOG1 1:100 diluted (Novocastra, Newcastle upon Tyne, United Kingdom).

Molecular analysis. For molecular investigations, representative tumor samples were isolated by microdissection, and the DNA was extracted following standard procedures. The *KIT* gene was analyzed by sequencing mutation hot spots (Exons 11, 9, 13, 14 and 17), while for the *PDGFRA* gene, the Exons 12,14 and 18 were analyzed as previously reported.[7]

In Patient A, a mutation consisting of a deletion of 12 bp affecting Exon 18 of *PDGFRA* (involving residues DIMH842–845) was detected. *KIT* resulted as wild-type for the hot spot exons examined.

Patient B resulted wild-type for *KIT*, whereas a point mutation in Exon 12 of *PDGFRA*, c.1682T>A, corresponding to the amino acidic mutation V561D was detected. Stem cell factor (SCF) detection by RT-PCR was performed as already described.[5]

Biochemical analysis. Biochemical analysis for KIT and PDGFRA expression and activation were performed as described elsewhere.[7,8]

Molecular modeling

All simulations were performed with the AMBER 9 suite of programs.[9] The 3D model structure of the PDGFRA, presently not available in the Protein Data Bank (PDB) structure repository, was built following a validate homology procedure[10] and refined using several energy minimization rounds, using the all-atom force field parameter sets parm99.[11] The imatinib molecule was then docked into the wild-type protein-binding site using Autodock 4.0[12] and the crystal structure of the KIT/imatinib complex as a template (code 1T46.pdb).[13] The resulting complex was further energy minimized to convergence. Eventual missing force field parameters for the inhibitor were taken from our previous work.[10,14]

The involved mutations were introduced into the wild-type structure of the corresponding PDGFRA/imatinib complex following a well-validated procedure.[10,14,15] Each mutant complex was then solvated and energy minimized using a combination of molecular dynamics (MD) techniques.[10,14] The 2-ns MD simulations at 37°C were then employed for system equilibration, and further, 4-ns MD were run for data production.

Following the MM/GBSA approach as described,[16–18] the affinity of wild-type and mutated PDGFRAs toward imatinib (ΔG_{bind}) was calculated as the sum of the electrostatic, van der Waals, polar salvation,[19] nonpolar salvation[20] and entopic contributions.[21]

Results

Radiologic evaluations after imatinib treatment

Both patients were evaluated by CT scan every other month, and tumor response was assessed by using Response Evaluation Criteria in Solid Tumors criteria. In both patients, the best response was a partial response. The size of the tumor was as follows:

Patient A (Fig. 1*a* and 1*b*) at the baseline 5.5 cm. On subsequent CT scans, the size of the tumor changed as here

Short Report

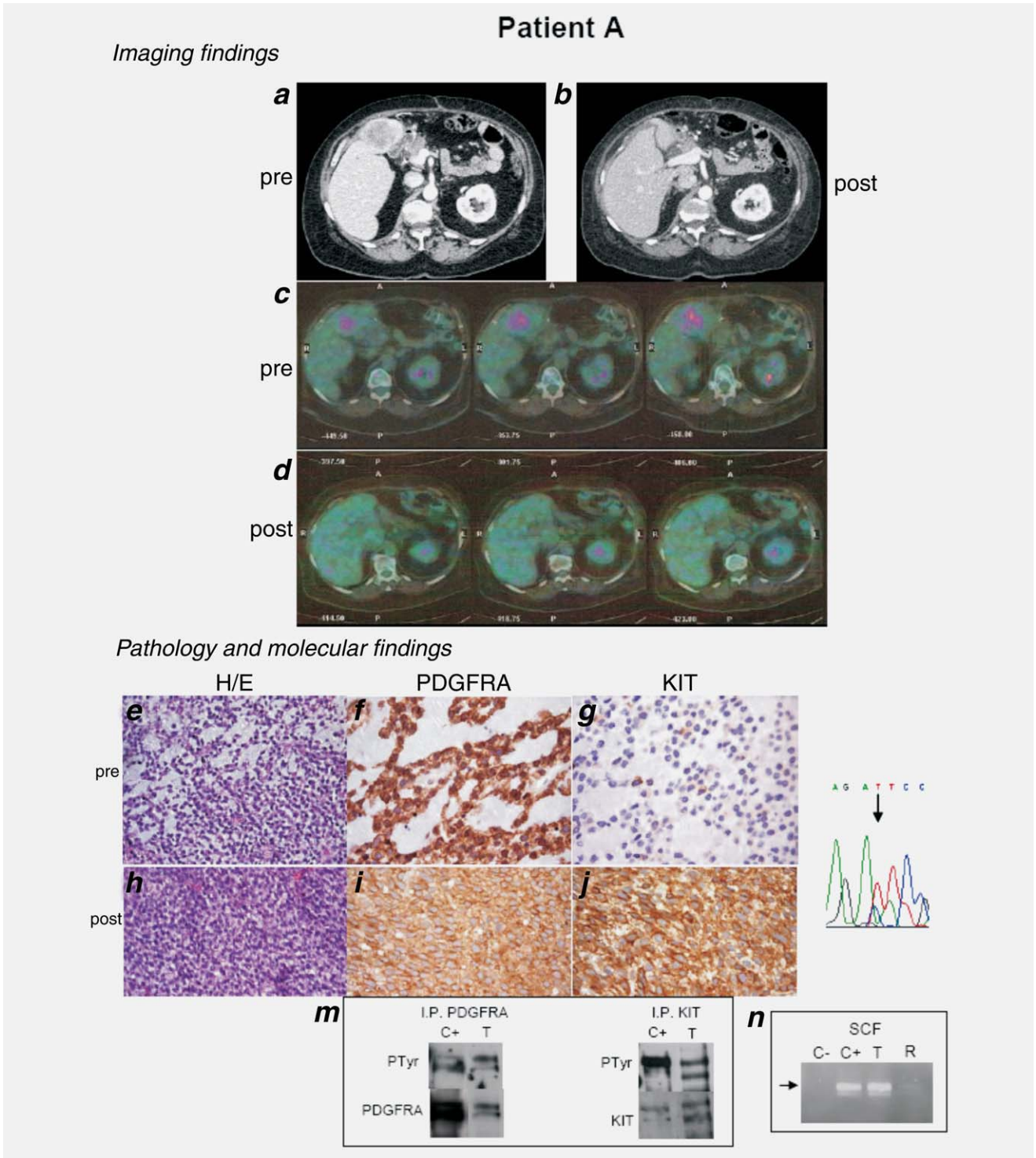

Figure 1. Patient A: CT before (*a*) and after (*b*) 8 months of imatinib. PET baseline (*c*) and after (*d*) 1 month of Imatinib. Pathology and molecular findings—pretreatment: (***e***) Epithelioid GIST, myxoid variant (H/E), (***f***) showing cytoplasmic and membrane PDGFRA and (*g*) KIT null immunophenotype, respectively, carrying *PDGFRA* DIMH842–845 in-frame deletion. Posttreatment: (*h*) The single cellular tumoral nodule, mainly made up of spindle cells (H/E), (*i*) retained PDGFRA immunostaining and (*j*) showed strong KIT immunostaining (*m*) both confirmed by biochemical analysis, which at molecular level, paralleled lacking of *KIT* mutations but (*n*) showed high level of SCF ligand when compared with a sample obtained from an highly regressive area (lane R).

Short Report

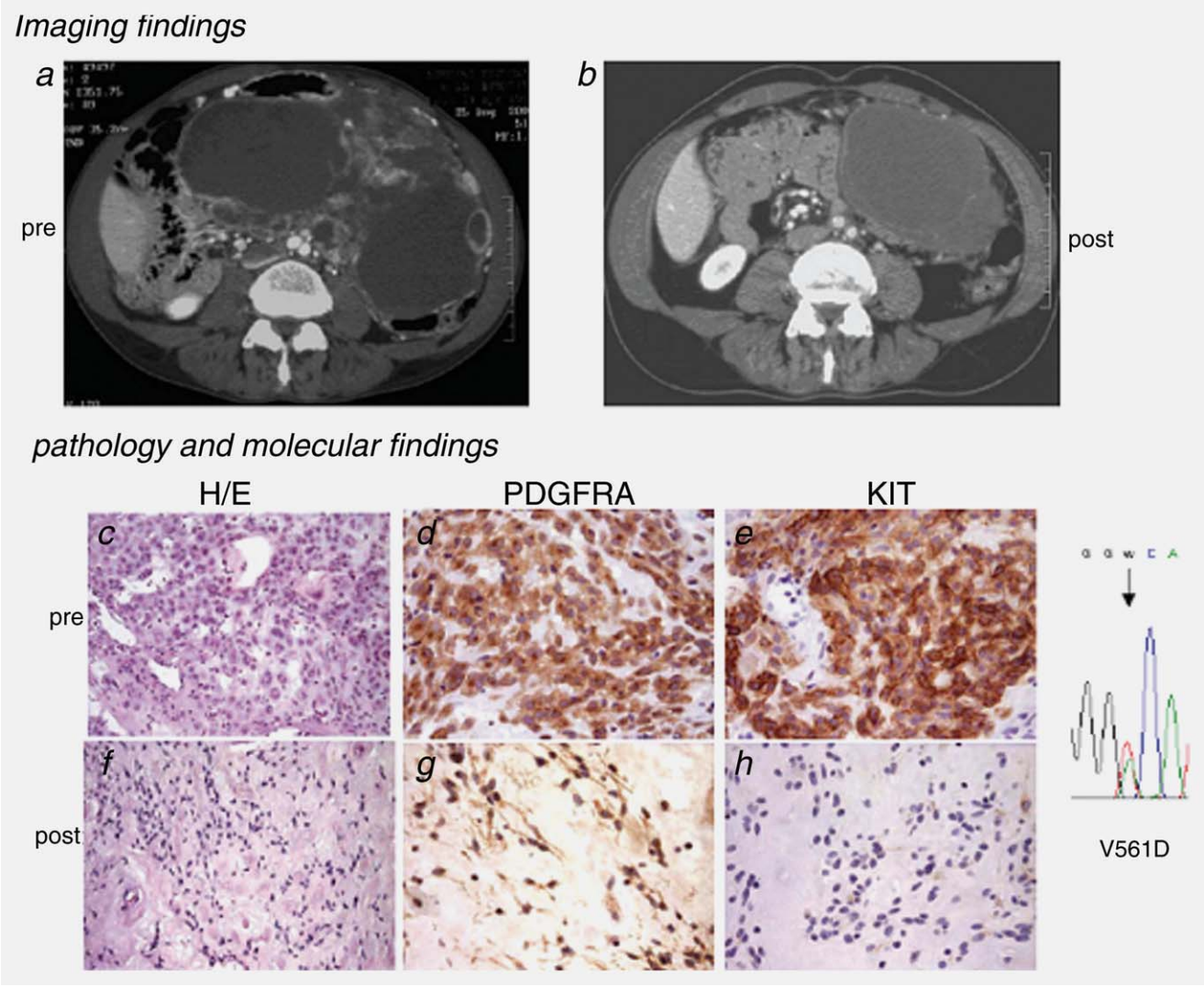

Figure 2. Patient B: CT before (*a*) and after (*b*) 6 months of imatinib. Pathology and molecular findings—pretreatment: (*c*) Epithelioid GIST, myxoid variant, true-cut biopsy (H/E), (*d*) showing dot-like PDGFRA immunostaining and (*e*) KIT expression, carrying *PDGFRA* V561D missense substitution. Posttreatment: (*f*) High regression rate of tumoral component was present throughout the surgical specimens (H/E). The residual cellularity, again spindle in shape, was (*g*) immunoreactive for PDGFRA and (*h*) very weakly for KIT.

Short Report

described: after 1 month of treatment: 4.5 cm; at 2 months: 3 cm; at 4 months: 2 cm; and at 8 months: 1 cm. Increased accumulation of [18F] FDG in the "abdomen" was seen on a PET scan obtained at the baseline (Fig. 1*c*). On a PET scan obtained 1 month after imatinib was started, decreased uptake was seen. Then, after 4 months, no abnormal uptake was seen to the tumor site, consistent with "cold" areas on CT scan (Fig. 1*d*).

Patient B (Fig. 2*a* and 2*b*) at the baseline 23 ($\times$ 21 $\times$ 11) cm. On subsequent CT scans, the size of the tumor was modified as here reported: after 6 weeks of treatment: 19 cm; at 4 months:16 cm; and at 6 months: 14 cm with a macroscopic report of 16 cm major diameter.

It is important to underline that in both the patient, no new lesions were observed.

Pretreatment and postimatinib treatment pathologic and molecular/biochemical assessment

Pathology

Patient A. The referred naive surgical resected primary tumor consisted of round epithelioid cells, with eosinophilic cytoplasm showing focally less cohesive pattern of growth with myxoid stroma, consistent with the so-called myxoid epithelioid GISTs[21] (Fig. 1*e*). The immunophenotype showed cytoplasmic and membrane PDGFRA immunoreactivity, coupled with null immunoreactivity for CD117 (Fig. 1*f* and 1*g*); DOG1 was also positive; the mitotic index was 40/50HPF and Ki-67 labeling $>$ 30.

After imatinib treatment, the patient underwent surgery. The postimatinib samples showed a high score[7,8,22] of

regression (residual viable tumor from <10% to <50%, no mitosis and no obvious Ki-67 immunostaining), represented by acellular areas characterized by the presence of eosinophilic proteinaceous matrix focally intermingled with ectatic vessels surrounded by hyaline sclerosis and scattered viable tumoral cells weakly immunoreactive for PDGFRA, DOG1 and KIT. The single highly cellular residual nodule of 0.5 cm, lacking regressive changes (Fig. 1*h*) retained PDGFRA and DOG1 immunoreactivity and, unexpectedly, revealed strongly immunoreactivity to CD117 (Fig. 1*i* and 1*j*).[23]

Patient B. The assessment of naive primary tumor was made by a true-cut biopsy (16 gouge). Again, the tumor consisted of discohesive epithelioid cells (H/E) placed in a myxoid stroma. Multinucleate tumor cells were also present (Fig. 2*c*). Tumor cells showed dot-like immunostaining for PDGFRA[6] and cytoplasmic and membrane immunostaining for KIT (Fig. 2*d* and 2*e*), in addition to DOG1 positivity.

The posttreatment surgical specimen showed a high score of regression with morphologic features superimposable with those described for Patient A (residual viable tumor from <10% to <50%, no mitosis and no Ki-67 immunostaining).[6] The very few residual viable cells revealed a pattern of spindle cell growth,[24] loosing the epithelioid morphology, but retaining a weak PDGFRA cytoplasmic immunoreactivity without dot-like pattern and DOG1 immunoreactivity but loss of CD117 (Fig. 2*g* and 2*h*).

Molecular and biochemical analyses

Patient A. Molecular investigation on the posttreatment regressed and not regressed areas revealed the primary Exon 18 *PDGFRA* mutation, whereas the nonresponsive residual nodule, showing CD117 immunoreactivity, investigated by sequencing for all *KIT* hot spots, did not show any mutation.[23]

The analyses, performed on residual nodule, demonstrated by biochemical analysis phosphorylated KIT and PDGFRA (lane T in Fig. 1, panel *m*), in keeping with IHC results and by RT-PCR analysis (Fig. 1, panel *n*) high levels of SCF, the KIT ligand (Fig. 1, lane T), when compared with a sample (Fig. 1, lane R) obtained from an highly regressed area (not shown).

Patient B. Also, in this case, the molecular analysis performed on a selected highly regressed area revealed the presence of the Exon 12 mutation, the V561D substitution. Unfortunately, the cryopreserved material was not suitable for the biochemical analyses.

Molecular modeling of the mutated PDGFRA receptors

MD simulations performed on a high quality 3D model of PDGFRA obtained by homology techniques (Fig. 3) revealed that both the Exon 18 deletion mutation DIMH842-845 and the Exon 12 missense mutation V561D do not negatively affect the affinity of the kinase for imatinib. The size-altering mutation DIMH842-845 is located in the activation loop of the second kinase domain of the receptor. Although involving the deletion of D842, a residue known to be critical for drug binding and, if mutate, causative of imatinib resistance, the exclusion of residue D846 (*i.e.*, the aspartic acid that follows H845 in the PDGFRA primary sequence) from this in-frame deletion has two major effects. First, it results in a conformational readjustment of the activation loop, which does not interfere with imatinib binding (Fig. 3*b*). Furthermore, it leaves this residual aspartic at codon 846 to play the role of controlling the swinging movement of the activation loop, This, in turn, is associated with a conformational shift of the ATP-binding pocket from the active conformation to the inactive one, to which imatinib binds selectively. In the case of the missense substitution V561D, although a small, hydrophobic residue is exchanged by a larger, negatively charged one, the position of the substitution and the relevant environment is such that this change is well tolerated in the juxtamembrane domain of the receptor (Fig. 3*c*). This, in turn, does not result in significant alterations of the inactive (or "closed") conformation of the kinase and, hence, of the imatinib binding site.

These pictorial evidences (Fig. 3) are clearly supported by the estimated free energy of binding (ΔG_{bind}) of imatinib to wild-type (Fig. 3*a*), DIMH842-845 (Fig. 3*b*) and V561D (Fig. 3*c*) mutated receptors reported in Table 1. As we can see from this table, both mutated receptors are predicted to have an affinity for imatinib comparable or slightly higher than that of the wild-type kinase. In fact, the free energy of binding differences between wild-type and each PDGFRA mutant and imatinib, $\Delta\Delta G_{bind}$, defined as:

$$\Delta\Delta G_{bind} = \Delta G_{bind}(\text{wild-type}) - \Delta G_{bind}(\text{mutant})$$

are both positive, indicating a favorable substitution or deletion at the considered positions, in line with the enhanced clinical response to therapy of the patient carrying this mutation.

Discussion

Herein, we report on two GIST patients with mutations of *PDGFRA* gene, respectively in Exon 18 (involving the deletion of DIMH842–845 residues) and 12 (V561D). Both patients responded clinically and pathologically to imatinib. Patient A after 27 months from starting therapy, and 19 from surgery, progressed and then started on sunitinib for 8 months with stable disease. Patient B is still on treatment with imatinib, without evidence of progression, after 3 year. Molecular modeling supported the sensitivity of the two mutations to imatinib.

These two *PDGFRA* mutations were already reported to be responsive to imatinib "*in vitro*." However, few and incomplete data were available on their "*in vivo*" sensitivity toward this inhibitor. In fact, only one patient with the deletion of the above reported residues in Exon 18 of *PDGFRA* mutation was indicated to be responsive to the drug in a single article.[24] Here, we confirm this anecdotal observation and add "*in vivo*" imaging and histologic evidence complemented

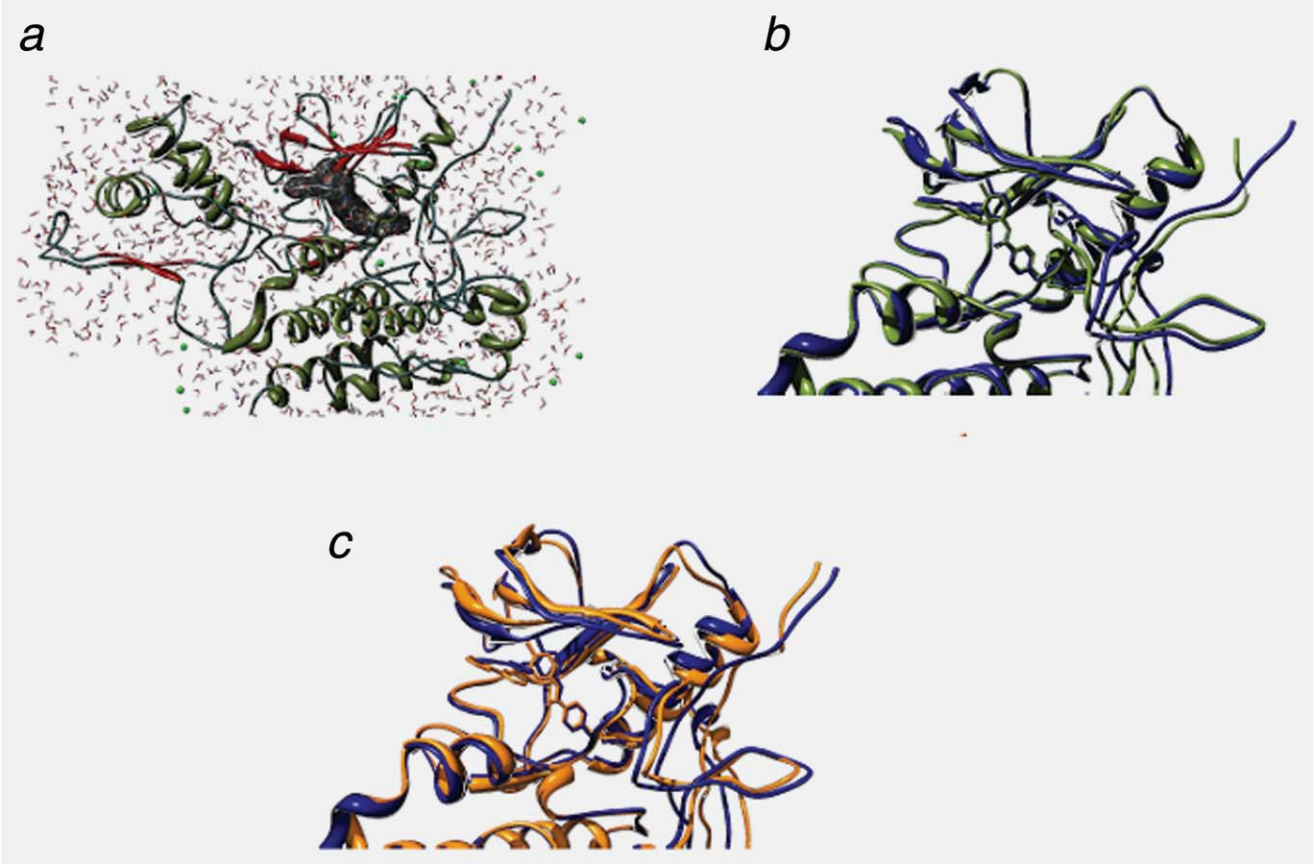

Figure 3. (*a*, left) MD simulations snapshot of the 3D structure of the wild-type PDGFRA in complex with imatinib. The secondary structure of the receptor has the following color code: dark olive green, helices; dark red, sheets; dark slate gray, turns and coils. Imatinib is in stick representation (atom color code: gray, carbon; red, oxygen; blue, nitrogen), with its van der Waals surface highlighted in dark gray (hydrogen atoms are omitted). Water molecules are represented as atom-colored lines. Chlorine and sodium counter ions are depicted as green and purple spheres, respectively. (*b*, right) Superposition of wild-type (blue) and DIMH842–845 *PDGFRA* mutant (olive green) in complex with imatinib. (*c*, bottom) Superposition of wild-type (blue) and V561D *PDGFRA* mutant (orange) in complex with imatinib. In (*b*) and (*c*) the inhibitor, in a protein-color stick representation. Hydrogen atoms, water molecules and counter ions are omitted for clarity.

Table 1. Calculated free energy of binding ΔG_{bind}, energy contributions to ΔG_{bind} and $\Delta\Delta G_{bind}$ for wild-type, DIMH842-845 and V561D mutant PDGFRA kinase domains and imatinib

PDGFRA	ΔG_{bind}	$\Delta\Delta G_{bind}$
Wild-type	−8.73	–
DIMH842-845	−9.62	0.89
V561D	−9.19	0.46

with modeling explanations for the sensitivity to imatinib of both ΔDIMH 842–845 and V561D *PDGFRA* mutated receptors.

Interestingly enough, in Patient A, after treatment, the only residual nonregressive area was a highly cellular, spindle cell tumoral nodule with high mitotic and Ki-67 rate and KIT immunoreactivity (Fig. 1*h*–1*j*). No *KIT* mutations were detected, whereas high levels of SCF were identified. These unexpected findings suggest that the tumor was genetically heterogeneous, made up of both a mutant population, which mostly vanished after treatment, and tumor cells with wild-type KIT that selectively survived. These findings reinforce the notion that, in the presence of strong inhibition of the oncogenic receptor,[8] (*e.g.*, PDGFRA as in this case), tumoral cells trigger alternative activation mechanisms (pathways) for survival, activating the homologous KIT receptor.[8] Consistently, in the residual nodule, in addition to activated PDGFRA, there was evidence of a ligand-dependent activation of KIT, as documented by the immunoprecipitation experiment, immunopositivity for both receptors and RT-PCR (Fig. 1*i*–1*n*). Furthermore, in both cases, the regressed areas (not shown) demonstrated few residual tumoral cells carrying *PDGFRA* mutations along with a low expression of PDGFRA. As for KIT, this was null in Patient B, whereas in Patient A, immunohistochemistry demonstrated KIT immunoreactivity in the very few, epithelioid featuring, residual tumoral cells, finding again in keeping with the escape tumoral mechanism by switching off PDGFRA.[8]

Short Report

Molecular modeling investigations were not provided previously for these mutations. Our simulation study showed that both the in-frame deletion DIMH842-845 and the missense substitution V561D do not result in decreased imatinib sensitivity for the kinase. In fact, from a structural standpoint, we observed that not only the two mutations do not negatively interfere with the conformation of the imatinib binding site but also the corresponding readjustments of the drug-binding pocket favor a better accommodation of the inhibitor within the kinase structure. Accordingly, the calculated affinities (ΔG_{bind}) of these mutant isoforms for the inhibitor are comparable or even higher than that of the wild-type receptor.

With regard to the PDGFRA Exon 18 DIMH842-845 mutation, it is interesting to note that a mutation involving the same location may have opposite effects with respect to imatinib inhibition, depending on the nature and context of the mutation itself (*e.g.*, deletion *vs.* missense). In fact, the missense substitution D842V (homologous to D816V in KIT receptor and associated to imatinib resistance), is associated with an ATP-binding pocket "open" conformation, which prevents response to imatinib resulting in unfavorable $\Delta\Delta G_{bind}$ values of −0.55 kcal/mol, 1.01 kcal/mol and 1.44 kcal/mol with respect to the wild-type, the DIMH842-845 and the V561D mutants, respectively. On the contrary, the deletion of the aspartic acid 842 contributes in keeping the pocket in a conformation favorable to imatinib binding (Tamborini and Pricl, personal communication).

In conclusion, we provided "*in vivo*" evidence that two mutations in *PDGFRA*, one in Exon 18 (involving deletion of residues DIMH842-845) and one in Exon 12 (V561D), are sensitive to imatinib and demonstrated that the employed molecular modeling results were able to yield a rationale for these clinical findings. Accordingly, the coupling of laboratory experiments and modeling investigations may constitute a powerful tool to predict imatinib sensitivity and help tailored clinical decisions in GIST mutations not yet functionally investigated.

References

1. Heinrich MC, Corless CL, Demetri GD, Blanke CD, von Mehren M, Joensuu H, McGreevey LS, Chen CJ, Van den Abbeele AD, Druker BJ, Kiese B, Eisenberg B, et al. Kinase mutations and imatinib response in patients with metastatic gastrointestinal stromal tumor. *J Clin Oncol* 2003;21: 4342–9.
2. Tamborini E, Bonadiman L, Greco A, Albertini V, Negri T, Gronchi A, Bertulli R, Colecchia M, Casali PG, Pierotti MA, Pilotti S. A new mutation in the KIT ATP pocket causes acquired resistance to imatinib in a gastrointestinal stromal tumor patient. *Gastroenterology* 2004;127: 294–9.
3. Sihto H, Sarlomo-Rikala M, Tynninen O, Tanner M, Andersson LC, Franssila K, Nupponen NN, Joensuu H. KIT and platelet-derived growth factor receptor alpha tyrosine kinase gene mutations and KIT amplifications in human solid tumors. *J Clin Oncol* 2005;23:49–57.
4. Corless CL, Schroeder A, Griffith D, Town A, McGreevey L, Harrell P, Shiraga S, Bainbridge T, Morich J, Heinrich MC. PDGFRA mutations in gastrointestinal stromal tumors: frequency, spectrum and in vitro sensitivity to imatinib. *J Clin Oncol* 2005;23:5357–64.
5. Perrone F, Tamborini E, Dagrada GP, Colombo F, Bonadiman L, Albertini V, Lagonigro MS, Gabanti E, Caramuta S, Greco A, Della Torre GD, Gronchi A, et al. 9p21 locus analysis in high-risk gastrointestinal stromal tumors characterized for c-kit and platelet-derived growth factor receptor alpha gene alterations. *Cancer* 2005;104:159–69.
6. Miselli F, Millefanti C, Conca E, Negri T, Piacenza C, Pierotti MA, Tamborini E, Pilotti S. PDGFRA immunostaining can help in the diagnosis of gastrointestinal stromal tumors. *Am J Surg Pathol* 2008;32: 738–43.
7. Miselli FC, Casieri P, Negri T, Orsenigo M, Lagonigro MS, Gronchi A, Fiore M, Casali PG, Bertulli R, Carbone A, Pierotti MA, Tamborini E, et al. c-Kit/PDGFRA gene status alterations possibly related to primary imatinib resistance in gastrointestinal stromal tumors. *Clin Cancer Res* 2007;13:2369–77.
8. Negri T, Bozzi F, Conca E, Brich S, Gronchi A, Bertulli R, Fumagalli E, Pierotti MA, Tamborini E, Pilotti S. Oncogenic and ligand-dependent activation of KIT/PDGFRA in surgical samples of imatinib-treated gastrointestinal stromal tumours (GISTs). *J Pathol* 2009;217: 103–12.
9. Case DA, Darden TA, Cheatham TE III, Simmerling CL, Wang J, Duke RE, Luo R, Merz KM, Pearlman DA, Crowley M, Walker RC, Hayik S, et al. AMBER 9, San Francisco: University of California, 2006.
10. Pricl S, Fermeglia M, Ferrone M, Tamborini E. T315I mutated bcr-abl in chronic myeloid leukemia and imatinib: insights from a computational study. *Mol Cancer Ther* 2005;4:1167–74.
11. Cornell WD, Cieplak P, Bayly CI, Gould IR, Kenneth I, Merz M Jr, Ferguson DM, Spellmeyer DC, Fox T, Caldwell JW, Kollman PA. A second generation force field for the simulation of proteins, nucleic acids, and organic molecules. *J Am Chem Soc* 1995;117:5179–97.
12. Morris GM, Goodsell DS, Halliday RS, Huey R, Hart WE, Belew RK, Olson AJ. Automated docking using a Lamarckian genetic algorithm and an empirical binding free energy function. *J Comput Chem* 1998; 19:1639–62.
13. Mol CD, Fabbro D, Hosfield DJ. Structural basis for the autoinhibition and STI-571 inhibition of c-Kit tyrosine kinase. *J Biol Chem* 2004;279:31655–63.
14. Tamborini E, Pricl S, Negri T, Lagonigro MS, Miselli F, Greco A, Gronchi A, Casali PG, Ferrone M, Fermeglia M, Carbone A, Pierotti MA, et al. Functional analyses and molecular modeling of two c-Kit mutations responsible for imatinib secondary resistance in GIST patients. *Oncogene* 2006; 25:6140–6.
15. Ferrone M, Perrone F, Tamborini E, Paneni MS, Fermeglia M, Suardi S, Pastore E, Delia D, Pierotti MA, Pricl S, Pilotti S. Functional analysis and molecular modeling show a preserved wild-type activity of p53C238Y. *Mol Cancer Ther* 2006;5:1467–73.
16. Kollman PA, Massova I, Reyes C, Kuhn B, Huo S, Chong L, Lee M, Lee T, Duan Y, Wang W, Donini O, Cieplak P, et al. Calculating structures and free energies of complex molecules: combining molecular mechanics and continuum models. *Acc Chem Res* 2000;33:889–97.
17. Srinivasan J, Cheatham TE III, Cieplak P, Kollman PA, Case DA. Continuum solvent studies if the stability of DNA, RNA, and phosphoroamidate-DNA helices. *J Am Chem Soc* 1998;120:9401–9.
18. Conca E, Negri T, Gronchi A, Fumagalli E, Tamborini E, Pavan GM, Fermeglia M,

Pierotti MA, Pricl S, Pilotti S. Activate and resist: L576P-KIT in GIST. *Mol Cancer Ther* 2009;8:2491–5.
19. Jayaram B, Sprous D, Beveridge DL. Solvation free energy of biomolecules: parameters for a modified generalized Born model consistent with the AMBER force field. *J Phys Chem B* 1998; 102:9571–6.
20. Weiser J, Shenkin PS, Still WC. Approximate atomic surfaces from linear combinations of pair-wise overlaps (LCPO). *J Comput Chem* 1999;20: 217–30.
21. McQuarrie DA. Statistical mechanics. New York: Harper & Row, 1976.
22. Sakurai S, Hasegawa T, Sakuma Y, Takazawa Y, Motegi A, Nakajima T, Saito K, Fukayama M, Shimoda T. Myxoid epithelioid gastrointestinal stromal tumor (GIST) with mast cell infiltrations: a subtype of GIST with mutations of platelet-derived growth factor receptor alpha gene. *Hum Pathol* 2004;35:1223–30.
23. Wong NA, Mangwana S. KIT and PDGFRalpha mutational analyses of mixed cell-type gastrointestinal stromal tumours. *Histopathology* 2007;51:758–62.
24. Heinrich MC, Corless CL, Demetri GD, Blanke CD, von Mehren M, Joensuu H, McGreevey LS, Chen CJ, Van den Abbeele AD, Druker BJ, Kiese B, Eisenberg B, et al. Kinase mutations and imatinib response in patients with metastatic gastrointestinal stromal tumor. *J Clin Oncol* 2003;21: 4342–9.